Environment-Friendly Deoxygenation of Non-Edible Ceiba oil to Liquid Hydrocarbon Biofuel: Process Parameters and Optimization Study

Nur Hafawati Binti Abdullah
Universiti Malaya
Nurul Asikin Asikin-Mijan
Universiti Kebangsaan Malaysia
Yun Hin Taufiq-Yap
Putra Malaysia University: Universiti Putra Malaysia
Hwai Chyuan Ong (ong1983@yahoo.com)
University of Technology Sydney
Hwei Voon Lee
Universiti Malaya

Research Article

Keywords: C8-C20 hydrocarbon, free fatty acid, green diesel, RSM, Alternative fuel, catalyst

Posted Date: August 5th, 2021

DOI: https://doi.org/10.21203/rs.3.rs-582604/v1

Version of Record: A version of this preprint was published at Environmental Science and Pollution Research on January 25th, 2022. See the published version at https://doi.org/10.1007/s11356-022-18508-4.

Abstract

Non-edible Ceiba oil has feasibility as a sustainable biofuel resource in tropical countries that act as alternative to a portion of the fossil fuels used today.Catalytic deoxygenation of the Ceiba oil (high O/C ratio) was conducted to produce hydrocarbon biofuel (high H/C ratio)over NiO-CaO_5/SiO_2-Al_2O_3catalyst with aims of high diesel selectivity and catalyst reusability. In the present study, Box-Behnken experimental design was used to evaluate and optimize liquid hydrocarbon yieldby considering following reaction factors: catalyst loading (1-9 wt.%), reaction temperature (300 - 380°C) and reaction time (30 -180 min). It was discovered that the optimum yield for hydrocarbon fractions*n*-(C_8 – C_{20}) was 77% under deoxygenation condition of 5 wt.% catalyst loading, reaction temperature of 340°C within 105 min. Besides, deoxygenationmodel indicated that interaction effects of catalyst loading-reaction time influence the deoxygenation activity greatly. Based on the product analysis, oxygenated species(e.g. CO_2 and CO) were removed mainly via decarboxylation/decarbonylation (deCOx) pathways. The NiO-CaO_5/SiO_2-Al_2O_3 catalyst is stable for five consecutive runs with hydrocarbon fractions within range of 66-75% and *n*-(C_{15}+C_{17}) selectivity of 64-72% as well. The stability profile of NiO-CaO_5/SiO_2-Al_2O_3 catalyst indicated that the catalyst able to maintain deoxygenation reactivity throughout five cycles with hydrocarbon yield of 66-75% and n-(C15+C17) selectivity of 64–72 %. However, coke deposition was noticed for the spent catalyst after several times of usage, which due to the high reaction temperature above 300 ^oC.

1. Introduction

Green diesel has potential as a bio-based hydrocarbon fractions for the blending with petrol-based diesel for the sake of sustainable and clean energy with climate change mitigation, that in line with sustainable development goals (goal 7 and goal 13) (Khan et al. 2015)(Shamanaev et al. 2020). The green diesel is renewable fuel that composed of petro-mimicked structures obtained from triglyceride-based plant oil conversion via deoxygenation (DO) processes (Rogers and Zheng 2019)(Asikin-Mijan et al. 2020a). The deoxygenation process involves both decarboxylation/decarbonylation (deCOx) pathways that produce diesel-range hydrocarbons from triglycerides and fatty acid derivatives by removal of CO_2/CO gas under inert condition (Pattanaik and Misra 2017)(Asikin-Mijan et al. 2020b).

The feedstock for green diesel recently focused on the utilization of non-edible feedstock, this is due to the food versus fuel issue and land degradation due to over agriculture crops plantation activity (Khan et al. 2015)(Abdulkareem-Alsultan et al. 2019)(Liu et al. 2012). Ceiba pentandra generally known as silk-cotton tree that highly available in Southeast Asia, India and Sri Lanka (Dharma et al. 2016). The ceiba pentandra also plays role as drought-resistant plant, which is easily growth in humid and tropical regions. The ceiba trees consisted of 25–28 wt.% of seeds with oil productivity of 11–28 %, which is 1280 kg/ha of oil(Ong et al. 2014). Ceiba oil is potential oils with production of 280516 million tonnes per annum but only few % is being utilized (Balajii and Niju 2020). Recently, ceiba pentandra oil (CPO) was selected for the production of renewable fuel such as biodiesel, yet it is believed that there is no studies focus on

process optimization for the production of CPO-derived green diesel by using response surface methodology (RSM) tool.

Catalyst is important to drive the deoxygenation reaction. Previously, we have reported the used of NiO-CaO_5/SiO_2-Al_2O_3 catalyst as effective catalyst for deoxygenation of triglycerides model compound (triolein) and real feedstocks (Asikin-Mijan et al. 2016b)(Asikin-Mijan et al. 2018). Based on those studies, the catalytic reactivity of NiO-CaO_5/SiO_2-Al_2O_3 catalyst was efficiently deoxygenizing various type of feeds (triolein, jatropha oil, waste cooking oil and palm fatty acid distillate) through selective deCOx pathways with 54–74% of *n*-(C_{15} + C_{17}) selectivity and hydrocarbon liquid yield of > 74%. Yet, this catalyst still exhibited higher affinity toward coking after reused multiples cycles with coke > 14 wt.%. It is believed that cracking and coking were motivated by existence of high unsaturated fatty acid species in the feedstock (FFA > 15%) (Abdulkareem-Alsultan et al. 2020)(Li et al. 2017). Considering this problem herein the cracking and the coking can be suppressed by utilization of low FFA feedstock such as CPO. Furthermore, the present study also highlights the optimization of CPO via RSM approach and the stability of the used catalyst investigated in detail.

2. Experimental

2.1 Materials

Nickel (II) nitrate hexahydrate ($Ni(NO_3)_2 \cdot 6H_2O$, > 99%) and calcium nitrate tetrahydrate ($Ca(NO_3)_2 \cdot 4H_2O$, > 99%) were obtained from R&M Company. Silica-alumina (SiO_2-Al_2O_3, grade 135) was procured from Sigma-Aldrich. The standard solvents and chemicals for gas chromatography (GC) analysis: alkane (C_8–C_{20}), nonene standard solutions and internal standard (1-bromohexane, > 98%) were purchased from Sigma-Aldrich. For GC solvent dilution, analytical grade *n*-hexane with purity > 98% was obtained from Merck. *Ceiba Pentandra* seeds were purchased from West Java, Indonesia. The CPO were extracted from its seeds via similar method reported by Ong et al. (Ong et al. 2013). The physicochemical properties and fatty acid composition of CPO were tabulated in Table 1.

Table 1
The physicochemical properties and fatty acid composition of CPO.

Oil properties	Value	Method
Acid value (mg KOH − 1)	11.9	AOCS Ca5a-40
FFA value (%)	5.9	AOCS Ca-5a-40
Fatty acid composition of oil (%)		AOCS Ce1-62 & Ce-661
Lauric (C12:0)	0.1	
Myristic (C14:0)	0.1	
Palmitic (C16:0)	19.2	
Palmitoleic (C16:1)	0.3	
Stearic (C18:0)	2.6	
Oleic (C18:1)	17.4	
Linoleic (C18:2)	39.6	
Linolenic (C18:3)	1.5	
Arachinic (C20:0)	0.56	
Malvaloyl C18:CE)	18.5	
Others	0.34	

2.2 Catalyst synthesis

The SiO_2-Al_2O_3 supported Ni-Ca oxides catalyst was synthesized via wet impregnation method, which is similar to our previous study (Asikin-Mijan et al. 2016b)(Asikin-Mijan et al. 2018). The catalyst support (SiO_2-Al_2O_3) was mixed to the metal salts solutions and stirred for 6 h under ambient conditions. The final mixtures then further dried at a temperature of 100°C in the oven. Then, the dried sample further ground into fine powder prior to calcine at a temperature of 500°C for 2 h under atmosphere condition. The catalyst was denoted as NiO-CaO_5/SiO_2-Al_2O_3.

2.3 Deoxygenation of CPO

The catalytic deoxygenation reaction of CPO was conducted in a 250 mL semi-batch reactor (Fig. 1). Approximately 10 g of CPO and selective amount of catalyst was added into reactor vessel. The deoxygenation process was performed under N_2 flow with respective reaction conditions that created by RSM tools (refer to Sect. 2.4).

2.4 Optimization design by Box-Behnken of RSM

Response surface methodology (RSM) with Box–Behnken experimental design was used to investigate the effects of different factors on deoxygenation of CPO and the interaction effects of factors towards the hydrocarbon yield response. Based on our former finding (Asikin-Mijan et al. 2017b), the three factors [catalyst loading (A), time (B) and temperature (C)] were identified as important parameters that highly influence the catalytic deoxygenation of CPO. The coded and uncoded levels of the independent parameters, as well as 17 runs of experimental design was depicted in Table 2 and Table 3, respectively.

Table 2
Box – Behnken coded and uncoded independent variables for optimization of ceiba oil over NiO-CaO_5/SiO_2-Al_2O_3 catalyst

Factors	Units	Level		
		-1	0	+1
A: Catalyst Loading	wt. %	1	5	9
B: Time	min	30	105	180
C: Temperature	°C	300	340	380

Table 3
Experimental design generated by RSM and responses from each reaction

No.	A:Catalyst Loading (wt.%)	B:Reaction Time (min)	C:Temperature (°C)	Hydrocarbon Yield (%)	
				Experimental response	Predicted response
1	1	30	340	79.01	71.89
2	9	30	340	74.60	75.41
3	1	180	340	66.09	65.28
4	9	180	340	25.00	45.52
5	1	105	300	71.39	78.30
6	9	105	300	83.43	72.02
7	1	105	380	65.25	76.67
8	9	105	380	70.63	63.71
9	5	30	300	74.39	85.00
10	5	180	300	70.98	64.86
11	5	30	380	73.53	79.64
12	5	180	380	70.89	60.28
13	5	105	340	72.26	73.54
14	5	105	340	75.23	73.54
15	5	105	340	73.40	73.54
16	5	105	340	74.50	73.54
17	5	105	340	74.10	73.54

2.5 Product analysis

Quantitative tests of produced CPO green diesel such as total hydrocarbon fractions ranged C_8–C_{20} (X_A, yield %) and selectivity of product carbon number (S_i, %) were determined by GC-FID (Shimadzu GC-14B) equipped with a HP-5 capillary column (length 30 m × inner diameter 0.32 mm × film thickness 0.25 μm) at analysis temperature of 300°C. The analysis condition and method of calculation was according to our previous study (Asikin-Mijan et al. 2019)(Asikin-Mijan et al. 2020c). For qualitative analysis that used to determine chemical composition of samples, both raw CPO and the CPO green diesels were characterised by using GC-MS (model SHIMADZU QP5050A) with a non-polar DB-5HT column (30m × 0.25 mm × 0.1 μm) that used a splitless inlet. The selectivity of the deoxygenated products was determine according to our previous study (Asikin-Mijan et al. 2019)(Asikin-Mijan et al. 2020c). The chemical functional group of

the CPO and CPO green diesel further determined by fourier transform infrared (FTIR) spectrometer Model: Perkin-Elmer (PS) equipped with a detector having a spectral range 300–3500 cm^{-1} with resolution 4 cm^{-1}.

3. Results And Discussion

In our previous study (Asikin-Mijan et al. 2018), the optimum condition for deoxygenation of triglycerides model compound (triolein) and realistic feedstock (WCO, JCO, PFAD) for green diesel production over NiO-CaO_5/SiO_2-Al_2O_3 catalyst were studied under N_2 flow atmosphere condition. Table 4 compilation of optimum condition data in experimental work that were done in this system. Due to an excellent achievement of the NiO-CaO_5/SiO_2-Al_2O_3 catalyst in optimizing the deoxygenation activity using 7 wt.% catalyst loading at 350 ^oC within 60 min, hence, this optimum condition was used as a basis to conduct optimization of CPO via RSM approach and the response of each experimental runs are depicted in Table 3. The suitability of quadratic model as well as the adequacy of the generated RSM model was explained in supplementary section.

Table 4
Summary from experimental studies conducted in semi-batch reactor under N_2 flow condition over NiO-CaO_5/SiO_2-Al_2O_3 catalyst [16].

Feedstock	FFA (%)	Optimum condition	Hydrocarbon yield (%)	*n*-(C_{15} + C_{17}) product selectivity
Triolein	2.5	Catalyst Loading: 7 wt.% Time: 60 min Temperature: 350 ^oC	92	61
WCO	18.4		87	54
JCO	15.4		74	80
PFAD	86.3		81	80

3.1 Interaction effect between deoxygenation parameters

The effect of the three reaction parameters towards the reactivity of deoxygenation process were presented in the form of three-dimensional (3D) response surface plot and contour plot. The presence of surface shape from 3D-surface plot indicated the effectiveness of interaction of two deoxygenation parameters towards the hydrocarbon yield and product selectivity. Meanwhile, the straightforward contour plot explains the overall nature of the response surface for the reaction model. Based on the interpretation from the model's plots, a narrow and precise range of optimum value corresponding to the high yield of hydrocarbon as well as product selectivity can be obtained (Kılıç et al. 2014).

Figure 2a-b shows the 3D response plot and 2D contour plot for interaction between catalyst loading (A) and reaction time (B) towards hydrocarbon yield, where the temperature is fixed at 340°C. Result shows that maximum hydrocarbon yield obtains more than 77% when the catalyst loading in the range 4.5 wt.%, and at time between ~ 70 min. Nevertheless, increment of catalyst amount along with reaction time

exhibit negative impact on the hydrocarbon yield. This agreed with negative interaction of AB in **Eq. S1**, which suggesting that simultaneous increase of both parameters will render negative impact on product yield. It was noted that reduced hydrocarbon yield at longer reaction time is caused by the unfavourable side reactions such as over-cracking or further polymerization of the deoxygenated liquid into lighter fractions. Additionally, longer reaction time reaction time will cause extensive catalyst deactivation due to coking, which in thus lowered deoxygenation activity (Pattanaik and Misra 2017).

Figure 2c-d displays 3D response surface plot and 2D contour plot of interactions between catalyst loading (A) and temperature (C) towards hydrocarbon yield, with reaction time at 105 min. Similar with above finding, high catalyst loading (> 7 wt.%) dramatically decrease the hydrocarbon yield. This phenomena was due to the excess of catalyst that resulted to mass transfer limitation between the oil and solid catalyst, which reduced the rate of deoxygenation process (Hermida et al. 2015). Based on the 2D contour plot, maximum hydrocarbon yield (77%) is achieved when 4.5 wt.% of catalyst were loaded into the reaction with reaction temperature ~ 320°C within 105 min. When comparing with data obtained in Fig. 2a-b, it clearly seen that reaction temperature plays an critical role in intensifying the kinetic reactivity of deCOx. The reaction model indicated that deoxygenation process was positively assisted at milder reaction temperature (320^{o}C).

The 3D response surface plot and 2D contour plot of interaction between reaction time (B) and temperature (C) of toward hydrocarbon yield using fix amount of catalyst loading (5 wt.% catalyst) were shown in Fig. 2e-f. Short reaction time and higher reaction temperature positively influence the deoxygenation activity. Notably, prolonging the reaction time in deoxygenation process does not improve the reaction activity and yield of product especially at intermediate temperature. High deoxygenation activity at higher reaction temperature was in agreement with Kubicka et al., (Kubičková and Kubička 2010), which yielded greater hydrocarbon yield when the reaction proceeded at higher reaction temperature. Similar finding also was reported by Pattanaik & Misra (Pattanaik and Misra 2017). Rich hydrocarbon obtained at high reaction temperature is highly correlated with the occurrence of cracking reaction via C-C bond cleavage (Ishihara et al. 2012). Whereby high cracking of CPO generally will lead to the formation of condensable reaction product which mainly comprised of short hydrocarbon fractions (gasoline: C_8-C_{12}) (Asikin-Mijan et al. 2017a). Based on the results generated from the Box-Behnken study, it can be concluded that optimum condition CPO deoxygenation toward formation of straight chain hydrocarbon fractions (77–81%) can be achieved at lower reaction temperature 300–340 ^{o}C, 5 wt.% catalyst loading and short reaction time ≤ 105 min.

Based on the curvatures nature of 3D surfaces in Fig. 2b, 2d and 2f, the results indicated that the mutual interaction of catalyst loading (A) with reaction time (B) was higher, as compared to the interaction parameters of AC and BC. Besides, the 3D surface plot revealed that the hydrocarbon yield varies remarkably with the increase of reaction time and catalyst loading. This revealed that most important variable in motivating the deoxygenation of CPO are reaction time and catalyst loading.

3.2 Product distribution profile for optimized hydrocarbon liquid product

To examine the predicted validity of Box-Behnken experimental design, the optimum condition of deoxygenation reaction of CPO over NiO-CaO_5/SiO_2-Al_2O_3 catalyst was performed under one optimized condition; reaction condition: 5 wt.% catalyst loading, 105 min at 340 ^oC under N_2 flow. Based on GC-FID analysis, the experimental result showed that the total hydrocarbon yield obtained is 75%, which is slightly less than predicted value from the reaction model (77%). The small degree of error (average of error = 2.2%) indicated the high accuracy of this deoxygenation model. It should be noticed that the liquid deoxygenated product also mainly diesel hydrocarbon fractions (*n*-(C_{15} + C_{17})) (72%) and minor of gasoline fractions *n*-(C_8-C_{12}) (Fig. 3a-b). As mentioned in Table 1, majority of fatty acid composition in CPO are C_{16} (palmitic acid – 9.2 wt.%) and C_{18} (oleic acid – 17.4 wt.% and linoleic acid – 39.6 wt.%). As shown in the product selectivity profile, the NiO-CaO_5/SiO_2-Al_2O_3 catalysed process rendered high deCOx selectivity with product favored of C_{n-1} hydrocarbons. As a result, *n*-C_{15} and *n*-C_{17} hydrocarbon fractions are dominant in the liquid hydrocarbon. GC-MS analysis was conducted to determine the chemical composition of deoxygenated liquid product. As shown in Fig. 3c, majority of compounds in the liquid product consist of alkanes and alkenes with carbon range of C_8 – C_{20} (selectivity ~ 77%), followed by alcohol which are E-11,13-Tetradecadien-1-ol, 1-Dodecanol and cis-7-Dodecen-1-yl acetate (selectivity 5.33%) and ketone (selectivity 0.47%). The chemical functional group of CPO and optimized deoxygenated liquid product is displayed in Fig. 3d. The FTIR spectra of CPO showed the chemical characteristics of triglyceride (vegetable oil), with five main absorption bands at 715 cm^{-1} (C-H stretch), 1160 cm^{-1} (C-O stretch, carbonyl ester), 1453 cm^{-1} (C-H bend), 1740 cm^{-1} (C = O, ester) and 2920 cm^{-1} (C-H bend). In the case of deoxygenated liquid product, result indicated shifting of absorption band from 1740 cm^{-1} (attributed to C = O of ester group in triglyceride) into the absorption band at 1709 cm^{-1} (attributed to C = O of carboxylic acid) (Asikin-Mijan et al. 2016a). Disappearance of C-O group from deoxygenated product strongly affirmed that the oxygenated species is removed during the reaction.

3.3 Stability and reusability of NiO-CaO_5/SiO_2-Al_2O_3

According to the literature (Lee et al. 2013), catalyst's reusability play critical role in determining the economical application of NiO-CaO_5/SiO_2-Al_2O_3 for for large-scale green diesel production. Due to this reason, the NiO-CaO_5/SiO_2-Al_2O_3 catalyst was reused for several runs under optimum deoxygenation condition at 340 ^oC, 105 min, and 3 wt.% catalyst loading under N_2. The catalyst was treated with hexane after each cycle, in oder to remove adsorbed organic materials followed by drying for 2 h in an oven. The results (Fig. 4a) indicated constant reactivity for five runs, which hydrocarbon yield was 75%, 71%, 70%, 69% and 66% for respective cycles, and the *n*-(C_{15} + C_{17}) selectivity of 64–72 % for the five consecutive runs. It was suggested that the occurrence of coke deposition on the catalyst's active sites during each

reaction cycles has resulted the marginal decrease of catalytic activity (Asikin-Mijan et al. 2020c)(Basyar et al. 2018).

The coke deposition of fresh and spent NiO-CaO_5/SiO_2-Al_2O_3 (after fifth runs) was investigated by using TGA analysis (Fig. 4b**)**. TGA profile indicated that fresh catalyst rendered minor weight-loss stage (5.01 ± 0.21%) at the temperature of 100–250°C, which attributed to decomposition of adsorbed water. Nevertheless, insignificant water weight loss is observed for spent catalyst, which suggesting multiple thermal deoxygenation process throughout the five runs facilitated the dehydration pathway, thus resulted in moisture-free NiO-CaO_5/SiO_2-Al_2O_3 catalysts (Communication et al. 2016). However, the spent catalyst showed significant second weight loss (23.2 ± 0.25%) at heating range of 300–600 ^oC that due to desorption of coke as CO or CO_2 (Asikin-Mijan et al. 2016b). Generally, the coke that desorbed at this range of temperature considered as “soft coke”, where the soft coke originates from the physicorbed carbonaceous or side product. Owing to the noticeable amount of coke formation on spent catalyst after five runs, hence it is strong affirmed that the reduction of the deoxygenation reactivity and deCOx product highly correlated with the coke deposited on the active sites of NiO-CaO_5/SiO_2-Al_2O_3 catalysts.

4. Conclusion

The study presented on the effect of deoxygenation parameters towards productivity of hydrocarbon fractions from non-edible CPO by using Box-Behnken-RSM tool. The deoxygenation model revealed that the most important variables to affect the process reactivity are reaction temperature and catalyst loading. Results indicated that NiO-CaO_5/SiO_2-Al_2O_3 catalysed process rendered optimal hydrocarbon yield (77%) and *n*-(C_{15} + C_{17}) hydrocarbon fractions (72%) at reaction condition of 340 ^oC, 105 min, 5 wt.% catalyst loading under N_2 flow condition. It was noted that the NiO-CaO_5/SiO_2-Al_2O_3 catalyst favor of high deCOx pathways, which produced majority of diesel-ranged fractions at C_{15} and C_{17}. The reusability profile explained that the NiO-CaO_5/SiO_2-Al_2O_3 catalyst was a stable catalyst with hydrocarbon yield within range of 66–75% and the *n*-(C_{15} + C_{17}) selectivity of 64–72 % throught five consecutive runs. However, undesirable coking deposition of catalyst occurred at deoxygenation process above 300 ^oC resulted slight decrement of hydrocarbon yield and *n*-(C_{15} + C_{17}) selectivity during each runs.

5. Declarations

Ethics approval and consent to participate

Not applicable

Consent for publication

Not applicable

Availability of data and materials

The datasets used and/or analysed during the current study are available from the corresponding author on reasonable request.

Competing interests

The authors declare that they have no competing interests.

Funding

The sources of funding provided by University of Malaya MOHE-Top 100 (IIRG)-IISS (IIRG002A-2020IISS) and Geran Galakan Penyelidik Muda (GGPM) 2020-15 were used for the purpose of design of the study and collection, analysis, and interpretation of data and in writing the manuscript.

Authors' contributions

Nur Hafawati Binti Abdullah: Investigation, Validation, Writing-Original draft. Nurul Asikin Mijan: Conceptualization, Writing-Review & Editing. Yun Hin Taufiq-Yap: Writing-Review & Editing, Resources. Hwai Chyuan Ong: Writing-Review & Editing, Resources. Hwei Voon Lee: Supervision, Funding acquisition, Project administration, Writing-Review & Editing, Resources. All authors read and approved the final manuscript.

Acknowledgements

The authors of this work acknowledge financial support for this project from University of Malaya MOHE-Top 100 (IIRG)-IISS (IIRG002A-2020IISS), as well as external technical support from Geran Galakan Penyelidik Muda (GGPM) 2020-15.

6. References

1. Abdulkareem-Alsultan G, Asikin-Mijan N, Lee H V., et al (2019) A Review on Thermal Conversion of Plant Oil (Edible and Inedible) into Green Fuel Using Carbon-Based nanocatalyst. Catalysts 9:1–25
2. Abdulkareem-Alsultan G, Asikin-Mijan N, Mustafa-Alsultan G, et al (2020) Efficient deoxygenation of waste cooking oil over Co 3 O 4 –La 2 O 3 -doped activated carbon for the production of diesel-like fuel . RSC Adv 10:4996–5009. https://doi.org/10.1039/c9ra09516k
3. Asikin-Mijan N, Lee HV, Juan JC, et al (2017a) Catalytic deoxygenation of triglycerides to green diesel over modified CaO-based catalysts. RSC Adv 7:46445–46460. https://doi.org/10.1039/C7RA08061A
4. Asikin-Mijan N, Lee HV, Juan JC, et al (2016a) Waste Clamshell-Derived CaO Supported Co and W catalysts for Renewable Fuels Production Via Cracking-Deoxygenation of Triolein. J Anal Appl Pyrolysis 120:110–120. https://doi.org/10.1016/j.jaap.2016.04.015

5. Asikin-Mijan N, Lee HV, Taufiq-Yap YH, et al (2016b) Optimization study of SiO2-Al2O3 supported bifunctional acid-base NiO-CaO for renewable fuel production using response surface methodology. Energy Convers Manag. https://doi.org/10.1016/j.enconman.2016.09.041
6. Asikin-Mijan N, Lee H V., Marliza TS, Taufiq-Yap YH (2018) Pyrolytic-deoxygenation of triglycerides model compound and non-edible oil to hydrocarbons over SiO2-Al2O3 supported NiO-CaO catalysts. J Anal Appl Pyrolysis 129:221–230. https://doi.org/10.1016/j.jaap.2017.11.009
7. Asikin-Mijan N, Lee H V., Taufiq-Yap YH, et al (2017b) Optimization study of SiO2-Al2O3 supported bifunctional acid–base NiO-CaO for renewable fuel production using response surface methodology. Energy Convers Manag 141:325–338. https://doi.org/10.1016/j.enconman.2016.09.041
8. Asikin-Mijan N, Ooi JM, AbdulKareem-Alsultan G, et al (2020a) Free-H2 deoxygenation of Jatropha curcas oil into cleaner diesel-grade biofuel over coconut residue-derived activated carbon catalyst. J Clean Prod 249:. https://doi.org/10.1016/j.jclepro.2019.119381
9. Asikin-Mijan N, Ooi JM, AbdulKareem-Alsultan G, et al (2019) Free-H2 deoxygenation of Jatropha curcas oil into cleaner diesel-grade biofuel over coconut residue-derived activated carbon catalyst. J Clean Prod Journal of:119381. https://doi.org/10.1016/j.jclepro.2019.119381
10. Asikin-Mijan N, Ooi JMM, AbdulKareem-Alsultan G, et al (2020b) Free-H2 deoxygenation of Jatropha curcas oil into cleaner diesel-grade biofuel over coconut residue-derived activated carbon catalyst. J Clean Prod 249:119381. https://doi.org/10.1016/j.jclepro.2019.119381
11. Asikin-Mijan N, Rosman NA, AbdulKareem-Alsultan G, et al (2020c) Production of renewable diesel from Jatropha curcas oil via pyrolytic-deoxygenation over various multi-wall carbon nanotube-based catalysts. Process Saf Environ Prot 142:336–349. https://doi.org/10.1016/j.psep.2020.06.034
12. Balajii M, Niju S (2020) Banana peduncle e A green and renewable heterogeneous base catalyst for biodiesel production from Ceiba pentandra oil. Renew Energy 146:2255–2269. https://doi.org/10.1016/j.renene.2019.08.062
13. Basyar K, Taufiq-yap YH, Hunns J, et al (2018) Mesoporous NiO / Al-SBA-15 catalysts for solvent-free deoxygenation of palm fatty acid distillate Microporous and Mesoporous Materials Mesoporous NiO / Al-SBA-15 catalysts for solvent-free deoxygenation of palm fatty acid distillate. Microporous Mesoporous Mater 276:13–22. https://doi.org/10.1016/j.micromeso.2018.09.014
14. Communication S, Romero M, Dalchiele EA (2016) Electrochemical Deposition of ZnO Nanorod Arrays onto a ZnO Seed Layer : Nucleation and Growth Mechanism. 11:8588–8598. https://doi.org/10.20964/2016.10.61
15. Dharma S, Masjuki HH, Ong HC, et al (2016) Optimization of biodiesel production process for mixed Jatropha curcas-Ceiba pentandra biodiesel using response surface methodology. Energy Convers Manag 115:178–190. https://doi.org/10.1016/j.enconman.2016.02.034
16. Hermida L, Abdullah AZ, Mohamed AR (2015) Deoxygenation of fatty acid to produce diesel-like hydrocarbons: A review of process conditions, reaction kinetics and mechanism. Renew Sustain Energy Rev 42:1223–1233. https://doi.org/10.1016/j.rser.2014.10.099

17. Ishihara A, Hashimoto T, Nasu H (2012) Large Mesopore Generation in an Amorphous Silica-Alumina by Controlling the Pore Size with the Gel Skeletal Reinforcement and Its Application to Catalytic Cracking. Catalysts 2:368–385. https://doi.org/10.3390/catal2030368
18. Khan TMY, Atabani AE, Anjum I, et al (2015) Ceiba pentandra , Nigella sativa and their blend as prospective feedstocks for biodiesel. Ind Crop Prod 65:367–373. https://doi.org/10.1016/j.indcrop.2014.11.013
19. Kılıç M, Pütün E, Pütün AE (2014) Optimization of Euphorbia rigida fast pyrolysis conditions by using response surface methodology. J Anal Appl Pyrolysis 110:163–171. https://doi.org/10.1016/j.jaap.2014.08.018
20. Kubičková I, Kubička D (2010) Utilization of triglycerides and related feedstocks for production of clean hydrocarbon fuels and petrochemicals: A review. Waste and Biomass Valorization 1:293–308. https://doi.org/10.1007/s12649-010-9032-8
21. Lee H V., Taufiq-Yap YH, Hussein MZ, Yunus R (2013) Transesterification of jatropha oil with methanol over Mg-Zn mixed metal oxide catalysts. Energy 49:12–18. https://doi.org/10.1016/j.energy.2012.09.053
22. Li Y, Zhang C, Liu Y, et al (2017) Coke formation on the surface of Ni / HZSM-5 and Ni-Cu / HZSM-5 catalysts during bio-oil hydrodeoxygenation. 189:23–31. https://doi.org/10.1016/j.fuel.2016.10.047
23. Liu Y, Sotelo-Boyás R, Murata K, et al (2012) Production of Bio-Hydrogenated Diesel by Hydrotreatment of High-Acid-Value Waste Cooking Oil over Ruthenium Catalyst Supported on Al-Polyoxocation-Pillared Montmorillonite. Catalysts 2:171–190. https://doi.org/10.3390/catal2010171
24. Ong HC, Masjuki HH, Mahlia TMI, et al (2014) Engine performance and emissions using Jatropha curcas, Ceiba pentandra and Calophyllum inophyllum biodiesel in a CI diesel engine. Energy 69:. https://doi.org/10.1016/j.energy.2014.03.035
25. Ong HC, Silitonga a. S, Masjuki HH, et al (2013) Production and comparative fuel properties of biodiesel from non-edible oils: Jatropha curcas, Sterculia foetida and Ceiba pentandra. Energy Convers Manag 73:245–255. https://doi.org/10.1016/j.enconman.2013.04.011
26. Pattanaik BP, Misra RD (2017) Effect of reaction pathway and operating parameters on the deoxygenation of vegetable oils to produce diesel range hydrocarbon fuels: A review Energy Reviews. Renew Sustain 73:545–557. https://doi.org/10.1016/j.rser.2017.01.018
27. Rogers KA, Zheng Y (2019) Decomposition of glucose with in situ deoxygenation in a low H2 pressure environment – Part I : Monometallic catalysts. Appl Catal A, Gen 569:75–85. https://doi.org/10.1016/j.apcata.2018.10.015
28. Shamanaev I V, Deliy I V, Gerasimov EY, et al (2020) Enhancement of HDO Activity of MoP/SiO2 Catalyst in Physical Mixture with Alumina or Zeolites. ctaalysts 45:1–13

Figures

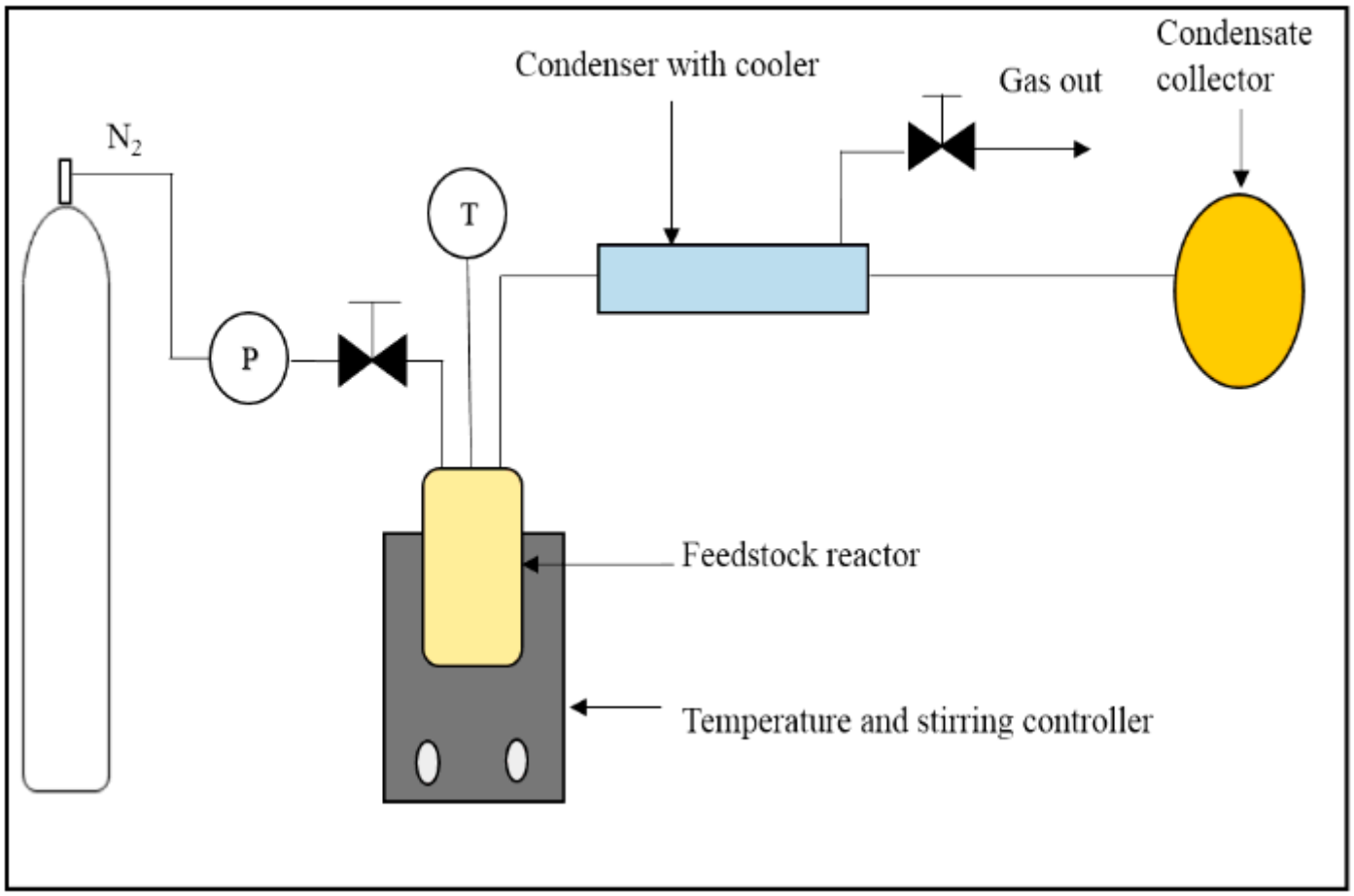

Figure 1

Schematic diagram for deoxygenation of CPO

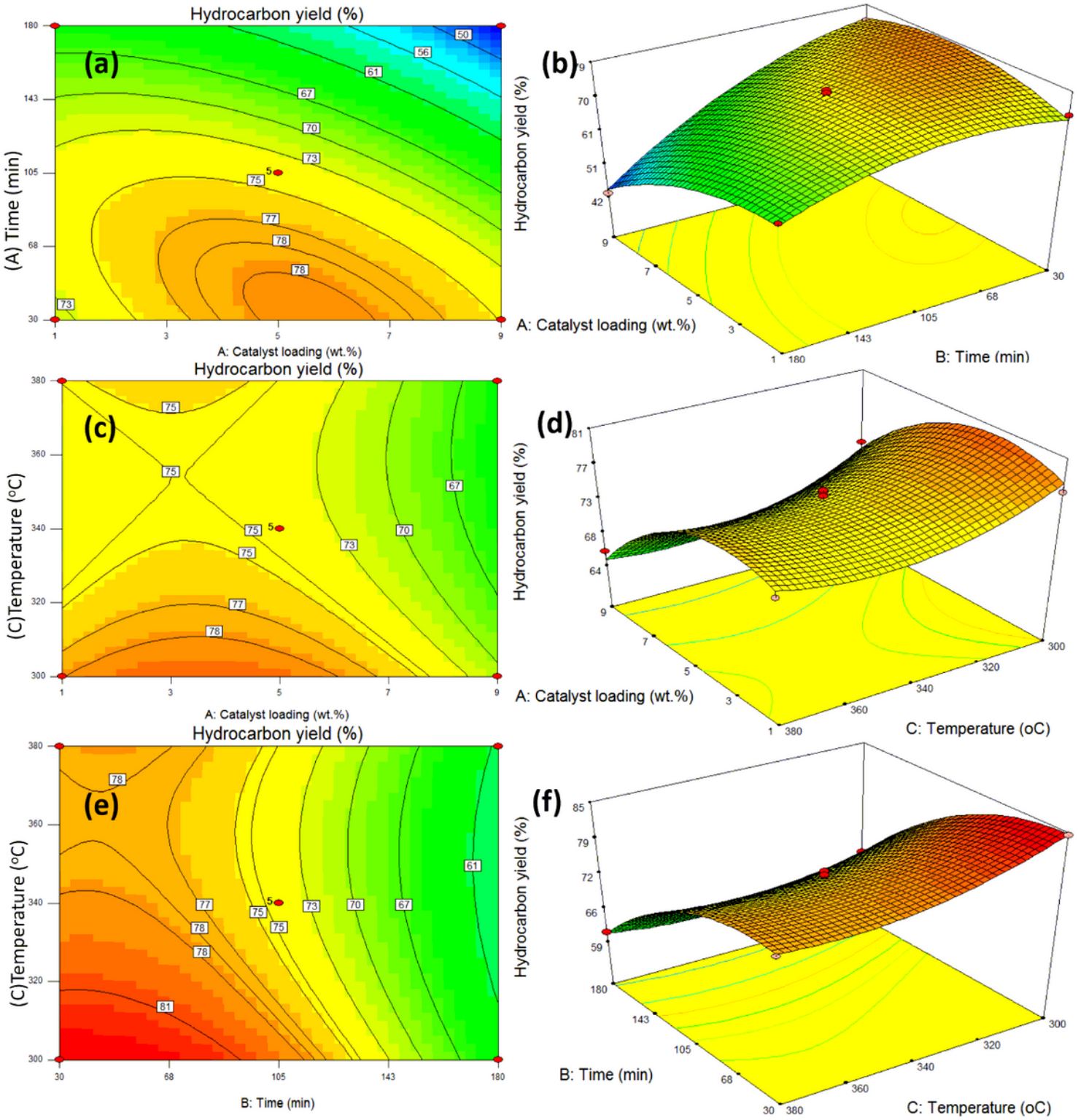

Figure 2

2D-contour plot and 3D-response surface plot and for (a) interaction of reaction time and reaction catalyst loading (AB), (b) interaction of reaction temperature and catalyst loading (AC), and (c) interaction of reaction temperature and reaction time (BC)

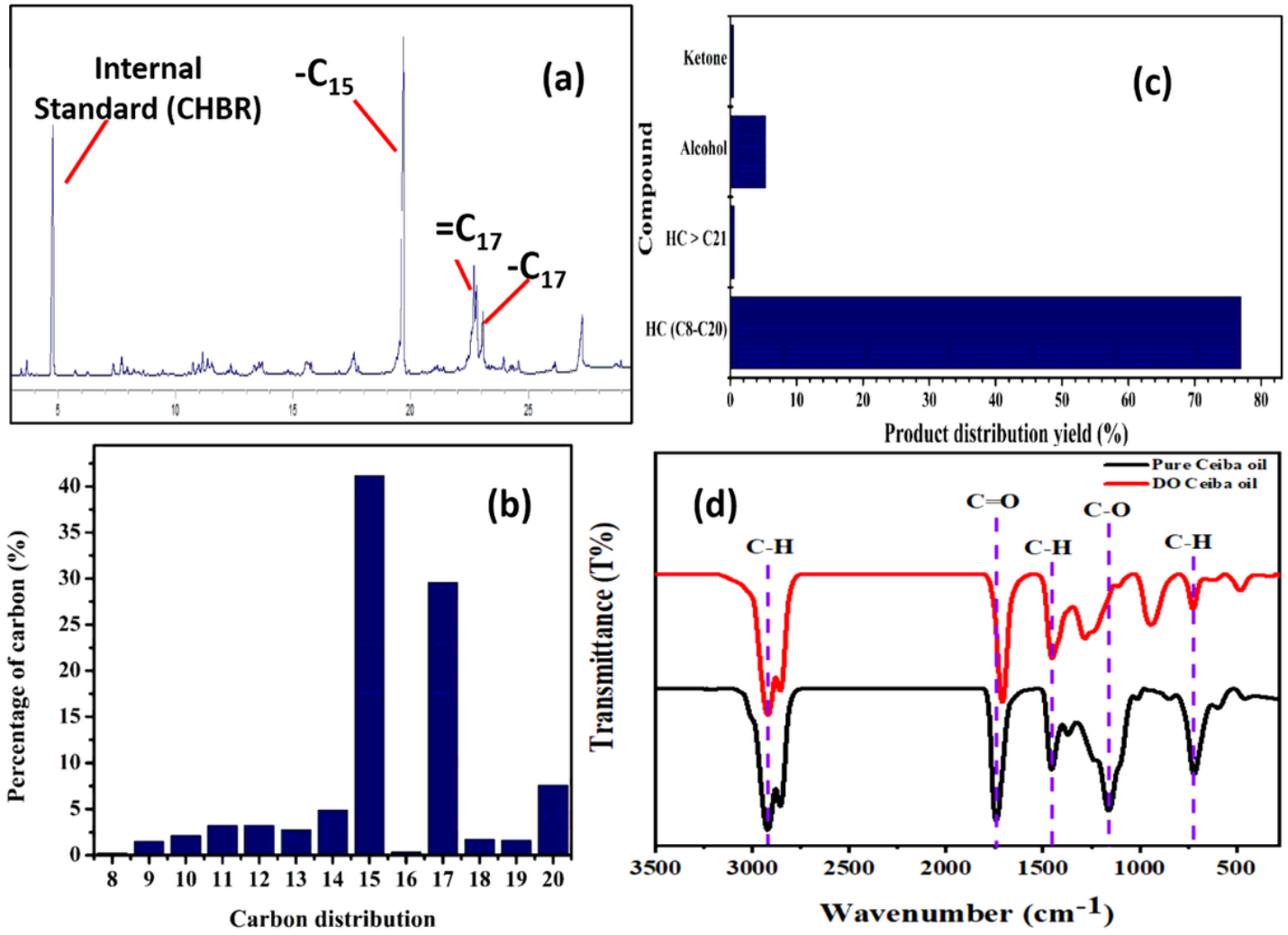

Figure 3

(a) GC-FID chromatogram and (b) carbon distribution for deoxygenated liquid under RSM optimum condition, (c) product distribution and (d) FTIR profile for deoxygenated liquid product and CPO. The reaction proceeded at optimum condition; catalyst loading: 5 wt.%, reaction time: 105 min and temperature: 340°C

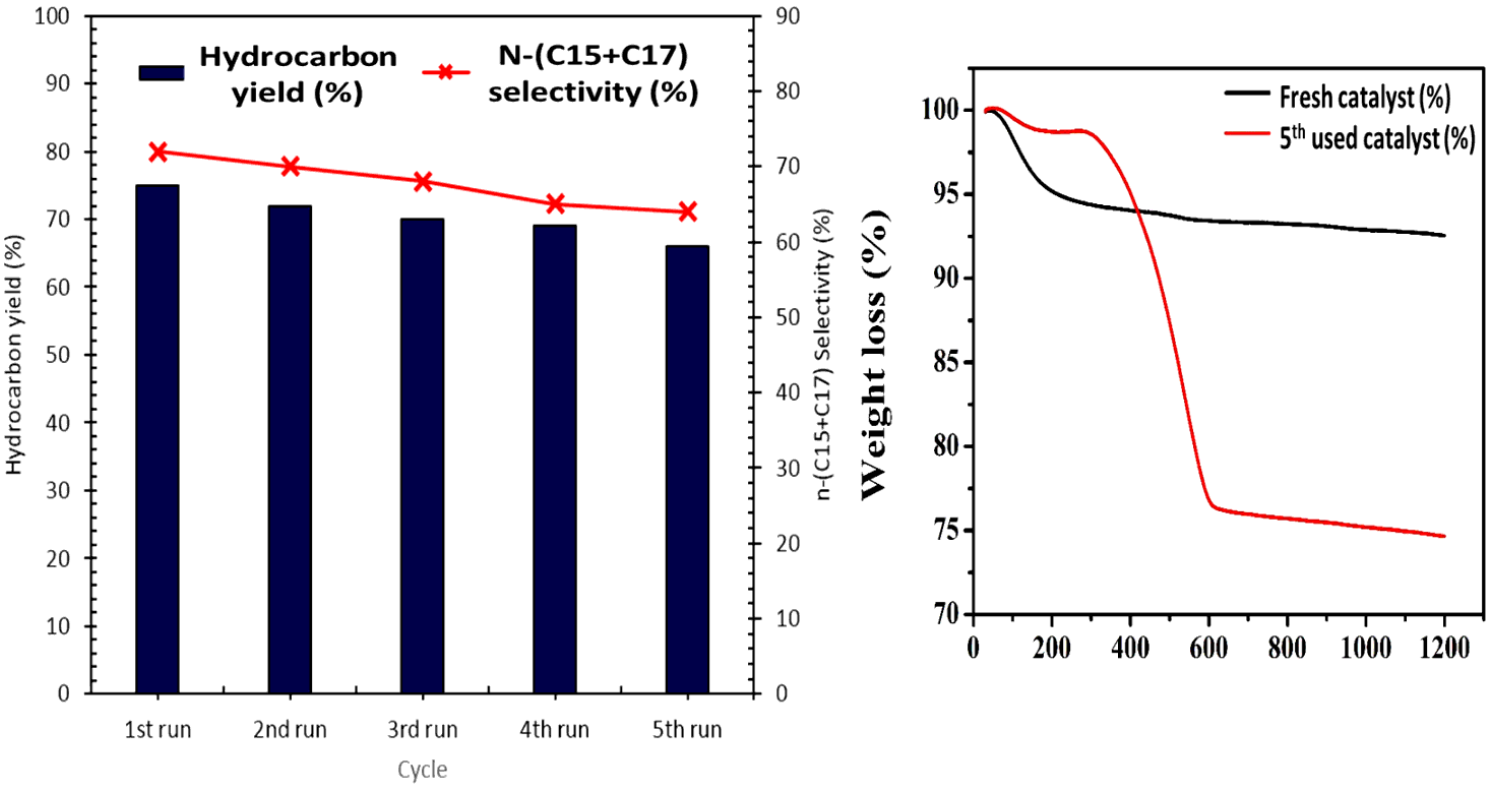

Figure 4

(a) Reusability of the NiO-CaO5/SiO2-Al2O3 catalyst towards straight chain hydrocarbon and (b) TGA profiles for fresh catalyst and 5th run used catalyst.

Supplementary Files

This is a list of supplementary files associated with this preprint. Click to download.

- Graphicalabstract2.docx